Calculation of retention curves for loams

J. Monnet
Gaiatech, 22 rue Antoine Chollier, 38170, Seyssinet

D. Mahmutovic, L. Boutonnier
EGIS Géotechnique, 3 rue Docteur Schweitzer, 38180, Seyssins, France

S. Taibi
LOMC, CNRS UMR 6294, Université Le Havre Normandie, BP540, 75058, Le Havre, France

ABSTRACT: Different approaches have been used for modeling retention curves. The experimental correlation was first proposed by Brooks and Corey (1966), Van Genuchen (1980) or Gallipoli et al. (2003). The physical modeling of non-saturated soils is used for this study. The shape of the retention curve is a consequence of the physical assumptions. The paper presents a theoretical model based on elastic spherical particle arrangement. Firsly, a uniform model is presented with a single diameter of soil particle. The second step extends the use of the model to graded soils. The model uses only physical parameters easy to measure. The model is compared with the experimental retention curve of three different samples of graded soils, glass sample (4μm-140μm), the Livet-Gavet loam (1.6μm-3mm) and the Jossigny Loam (0,1μm-0,1mm). It shows its ability to model the experimental curves. It is of great interest for engineers as it gives a retention curve without direct measurements of suction

1 INTRODUCTION

Development of numerical calculations and increasing power of microcomputers allow the determination of the behaviour of large soil constructions such as levees, embankments, road earthworks. All these earth structures are compacted at Proctor optimum with a degree of saturation between 80 to 98% with an unsaturated soil. For a precise estimation of the final state of density of the soil, it is necessary to model the compaction of the soil along a wetting path. Furthermore, when the construction of the earth structure is completed, it sustains drying and wetting events associated to rainy and sunny conditions. These events therefore require the development of a model able to simulate drying and wetting paths

There are several ways for modelling retention curves. The first method is to use experimental relationships. This approach (1) has many successes with the Brooks and Corey's model (1966) which needs the determination of air entry suction s_{air} and the experimental parameter δ. Later Van Genuchen (1980) used a new experimental relationship (2) able to simulate larger retention curves with 3 experimental parameters (α, n, m). Gallipoli et al. (2003) followed the same research scheme and proposed a complete experimental relation (3) with 4 experimental parameters (Φ, Ψ, n, δ).

The second method is to consider physical modelling. With this approach, there is no need to assume particular shapes of the retention curves, which is a consequence of the physical assumptions. One option is to consider the soil as a porous medium (Or and Tuller, 1999). The second option is to consider the soil as a structure made of spherical particles, as used in this paper. The present study focuses on a theoretical model based on elastic spherical particle arrangement. This approach follows a new research way so that the physical phenomenon can be explained whilst the number of experimental parameters is limited.

$$S_r = \left(s/s_{air}\right)^{-\delta} \quad (1)$$

$$S_r = \left(1+\left[a.s\right]^n\right)^{-m} \quad (2)$$

$$S_r = \left(1/\left[\Phi.\left(\upsilon-1\right)^{\Psi}.s\right]\right)^{-\delta} \quad (3)$$

2 THE EXPRESSION OF THE THEORETICAL RETENTION CURVE FOR UNSATURATED SOIL

2.1 *Hypothesis*

Many authors have mentioned the existence of four areas of saturation, each with a distinct behavior. This assumption is resumed in the design of our model, mostly based on the work of Boutonnier (2007).

- Domain D1 : $s \geq s_{air}$ and $S_r \leq S_{rair}$

The gaseous phase is continuous in the soil. This state gives a suction s higher than the air entry

suction and a lower degree of saturation than the degree of saturation of air entry.

- Domain D2 : $s \leq s_{air}$ and $S_{rair} \leq S_r \leq S_{re}$ and $u_w \leq 0$

In this domain, free air disappears. The air is occluded in the soil. The air is in contact with the soil particles. The suction has the effect of increasing the strength of interparticle contacts. The water pore pressure is negative

- Domain D3 : $S_{re} < S_r < 1$ and $u_w > 0$

Air is occluded into the soil sample and is considered to be independent from the skeleton. Capillary strength has no effect on the contact forces between soil particles. We consider here D3 is corresponding with the case of positive pore pressures with a degree of saturation lower than 1.

- Domain D4 : $S_r = 1$

There is no air in gaseous state in the soil. The soil is saturated. The boundary between D3 and D4 can also be expressed through the pore pressure with a degree of saturation equal to 1.

2.2 *Deformation of the spherical particles and volume of meniscus: Domain D1*

To complete the original model of non-saturation (Monnet and Boutonnier, 2012) written for domain D2 to D4, it was decided to model the D1 domain.

Under the action of the water at the interparticle contact, there is suction on the cross section of the meniscus (Fig.1) and surface tension (Taibi, 1994). The model of soil is composed of uniform spherical particles of radius R. According to Laplace's law, suction is the product of the surface tension T_c by the sum of two principal curvatures of radius r of the meniscus and the radius b of the torus corresponding to the wetted area (4). Under the action of a normal force F_N (5) on the contact plane, the two balls deforms elastically. The detail of these calculations is presented in Monnet et al. (2017).

$$s = T_c.(1/r - 1/b) \quad (4)$$

$$f_N = s.\pi.b^2 + 2.\pi.b.T_c \quad (5)$$

2.3 *Analytical calculation of meniscus volumes with a wetting angle : Domain D1*

The contact between the particles and the water has a wetting angle of θ_c which varies in case of drainage or humidification (Gras, 2011).

The calculation of the volume of the meniscus is made with a rotational assumption around the horizontal axis through the centre of the two particles (Fig. 2) and a relative horizontal symmetry with the EC plane contacting the particles. The volume of the meniscus is the difference between the volume of CDAE frustum, the volume of the soil flattened sphere CDAB, and the volume of air of the torus of AFE area (6). Monnet et al. (2017) present the calculation of the menisci volume.

$$V_{men} = 2.(V_t - V_p - V_{air}) \quad (6)$$

The meniscus volume is simulated by a Solidworks® model which allows measuring the numerical volume of the meniscus, and comparing with the analytical value of the meniscus. The comparison shows that the analytical relations allow finding the meniscus volume of the Solidworks® model.

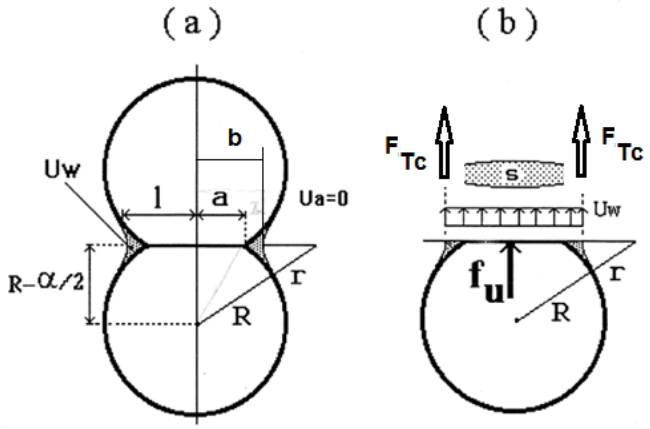

Figure 1. Theoretical meniscus model between two spheres (S.Taïbi, 1994)

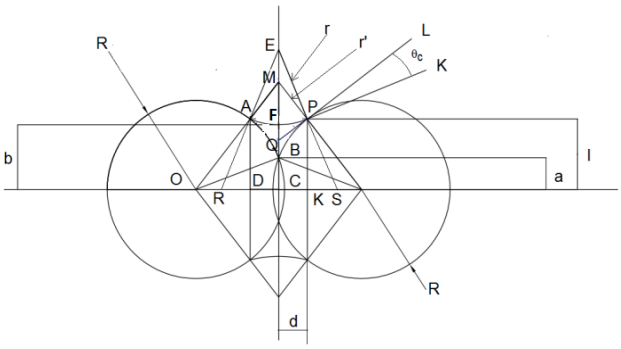

Figure 2. Geometrical model for the meniscus calculation of 2 spherical particles with a wetting angle θ_c (Monnet et al., 2017)

2.4 *Arrangement of soil particles*

The different arrangements of uniform soil particles give a variation of void ratio between 1.315 to 0.343 (Taibi, 1994). The SoildWorks® program was used for the precise modeling of the four possible arrangements, tetrahedral, cubic, octahedral, dodecahedral (Fig.3 to 6). It shows that the void ratio is independent of the radius of the particles, but depends only on the arrangement between particles. The radius of particles has only an influence on the size of the REV (Representative Elementary Volume). The variables which describes the different phenomenons along the drying path are the ratio between the air bubble and the particles radius. The Solidworks model allows determining into the REV:

- The number, the angle of contact for each particle
- The number of total menisci per arrangement

For the drying path, the model finds:

- The radius of the bubble appearing at nucleation
- The number of bubbles able to appear inside VER
- The degree of saturation at nucleation
- The suction at nucleation
- Radius and suction of the percolating bubble

For the wetting path, the model finds:

- The radius of the bubble which percolates
- The suction at percolation

The theoretical calculation of the meniscus can be performed when the menisci are independent. When the meniscuses merge, it is assumed that the suction remains unchanged.

Figure 3. Tetrahedral arrangement, e = 1.315 ; 4 contacts per particle ; 8 menisci

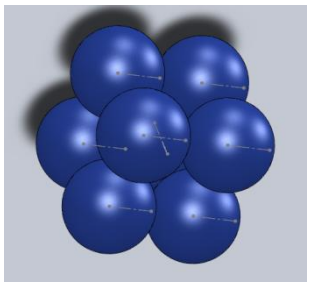

Figure 4. Cubic arrangement ; e = 0.910 ; 6 contacts per particle ; 3 menisci

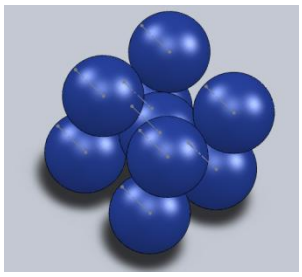

Figure 5. Octahedral arrangement ; e = 0.470 ; 8 contacts per particle ; 8 menisci

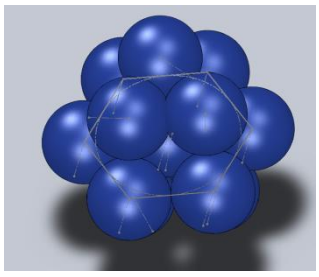

Figure 6. Dodecahedral arrangement ; e = 0.343 ; 12 contacts per grain ; 17.6 menisci

2.5 *Theoretical retention curve for a uniform soil: Domain D1*

$$V_w = S_r.e.REV/(1+e) \quad (7)$$

$$V_{men} = S_r.r.REV/[(1+e).Nb_{menisci}] \quad (8)$$

For a uniform soil, with only one diameter of soil particles, there are different possible arrangements (tetrahedral, cubic, octahedral, dodecahedral) where the relative position of the particles is known as well as the REV, the void ratio, the number and orientation of the contacts in the arrangement are known.

On a reverse way, the knowledge of the void ratio allows the type of arrangement of the soil particles to be known. The knowledge of the water content or the saturation allows the calculation of the total volume of water in the REV (7). The knowledge of the number of contacts in the REV and the number of complete menisci allows the calculation of the volume (8) of a single meniscus (Monnet et al., 2017). The volume of the meniscus depends on the radius of the meniscus, the radius of the grain and the suction. This allows the calculation of the suction associated with a void ratio and water content.

2.6 *Compactness and homogeneity of granular mixture for a graded soil*

The theoretical model is organized from the larger to the smaller of n different D_i diameters for the soil skeleton particles, such as (9). The symbol C is the compactness which is equal to the solid volume of the soil sample (10). The relative compactness to the total sample of the class i is noted C_i (11). As a consequence, the total compactness C of the soil sample is given by (12). In the theory, R_i corresponds to the volume refusal on the sieve of diameter D_i , based on the total volume of the sample grains (13). Assuming a single density for all aggregates, this term is the refusal by sieve reduced to the total mass of the sample.

$$D_1 \geq ...D_i... \geq D_n \quad (9)$$

$$C = V_s/V_t = 1-n \quad (10)$$

$$C_i = V_{si}/V_t = 1-n_i \quad (11)$$

$$C = \sum_{i=1}^{n} C_i \quad (12)$$

$$R_i = C_i \Big/ \sum_{j=1}^{n} C_j = M_{di} \Big/ \sum_{j=1}^{n} M_{dj} \quad (13)$$

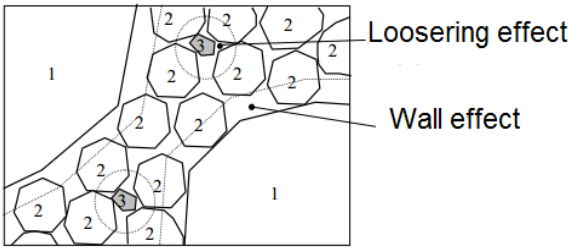

Figure 7. The perturbations exerted on the middle class grains by the large grains and the small grains (De Larrard, 1999).

2.7 *Mixture scattered - general case for a graded soil*

The mixture of 3 parts is subjected to a decompacting effect by small grains (grains 3 Fig.7) on the larger ones (grain 2 Fig.7) and a wall effect of the coarse grains (grain 1 Fig.7) on the smaller ones (grain 2 Fig.7).

This can be generalized for n different classes by finding the virtual C compactness of the mixture, considering that the class i is dominant in equation (14-15). The relative density corresponds to β_i which is the ratio between the density of the homogeneous mixture of rank i and the density of the solid part of the soil. The experimental β_i coefficient is found (16) by interpolation of the experimental curve (Fig.8) which is the evolution of density of the

homogeneous sample of a different diameter compacted with a standard energy.

$$C = Inf_{1\le i\le n} C_i \quad (14)$$

$$C_i = \beta_i \Big/ \left[1 - \sum_{j=1}^{i-1} \left(1 - \beta_i + b_{ij}.\beta_i.\left[1 - 1/\beta_j\right]\right)\right] \quad (15)$$

$$\beta_i = \rho_{di}/\rho_s = -0.0315.(LogD_i)^2 - 0.135.LogD_i + 0.486 \quad (16)$$

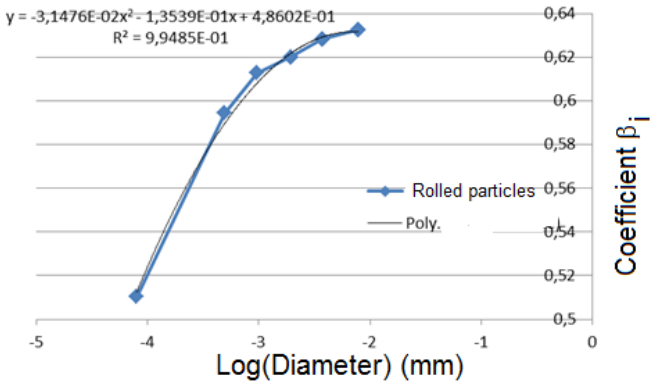

Figure 8. βi compactness coefficient of rolled grains (De Larrard, 1999)

2.8 *Compactness of each size class : graded soil*

In a mixture of n different diameter organized according to equation (9) from the largest to the smallest, the theory of De Larrard (1999) allows the diameter D_i dominant, with its compactness to be found, which allows calculation of the porosity of class i of grains by equation (11) and the corresponding void ratio e_i.

In the first step of the calculation, the total compactness C_m of the mixture and the porosity n_m are known. On the total size curve (Fig.9). The dominant diameter separates the curve into two portions:

- At the right of the dominant diameter, large elements floating into small elements
- At the left of the dominant diameter, small particles fall into the gaps left by the dominant grains

Each portion has a density of its own and depends only on the prevailing diameter. Then we can consider two separate samples for which two new dominant diameters appear with their own characteristics of compactness, porosity and void ratio. We can determine from part to part all theoretical porosity of all diameters of the particle curve size.

Let us consider the total mixture of n different particles. For a single rank of aggregate i, the volume of the void V_{vi} in the mixture is given by the equation (17). Under these conditions, the void ratio e_{Theo} of the theoretical mixture is known (18). This void ratio is different from the measured void ratio e_{Test} since the former refers to a standardized method of compaction. We assume the proportionality between the void ratio of the different classes. According to equation (19) e_{Test} is the known value of mixture measured during the test; e_{Theo} is the void ratio of the mixture compacted at the standard energy, and e_{mi} is the void ratio of each diameter in the compacted sample. This void ratio e_{mi} allows knowing the arrangement of the particle class.

$$V_{vi} = e_i.R_i = n_i.R_i/(1-n_i) \quad (17)$$

$$e_{Theo} = e_m = V_v \Big/ V_s = \left(\sum_{i=1}^{n} n_i.R_i/[1-n_i]\right) \Big/ \sum_{i=1}^{n} R_i \quad (18)$$

$$e_{mi} = e_{Test}/e_{Theo}.e_i \quad (19)$$

$$w_{NS} = \rho_w \Big/ \rho_s.\left(w.\rho_w \Big/ \rho_s - \sum_{j=i}^{n} e_{mi}.R_i\right) \quad (20)$$

$$S_s = 0.01.(VBS/319.87).A_v.A_{MB} \quad (21)$$

$$\varphi_a = (S_{Part}/\rho_d)/S_s \quad (22)$$

$$S_s = \left(\sum_{i=0}^{n} [S_{Partsi}.R_i]/\rho_{di}\right) \Big/ \varphi_a \quad (23)$$

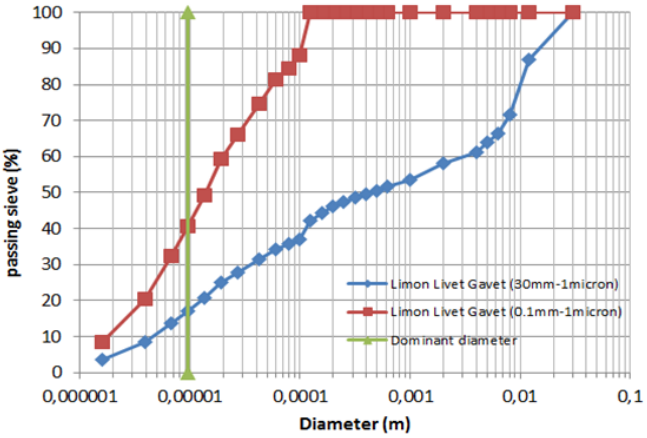

Figure 9. The grade curve of Livet-Gavet loam separated into two portions, large elements on the right and left small particles

2.9 *Grain diameter at the air inlet on wetting path*

We assume that small pores are saturated (S_{ri} = 1), and that large pores are dry (S_{ri} = 0). Under these conditions, the water content can be decomposed as a function of particle size (20), with dry pores (S_r = 0) for j <i (large diameter) and saturated pores (S_r = 1) for j> = i (small diameters). The rank of the pores involved in the air inlet is i. In the relation (20), the only unknown is the rank i. The knowledge of e_{mi} , R_i and the water content w_{NS} allows the rank i of the air inlet and the suction of class i, to be found.

2.10 *Suction at the air entry on drying path*

The model assumes that the air begins to percolate through the soil when the bubble can pass through the smallest porosity of the class of particles. For lower water content the relation between degree of saturation and suction follows the logarithm expression (1) where δ is an inner parameter of the model.

2.11 *Specific surface of the soil*

The specific surface of the soil S_s can be measured with the Methyl Blue Test and the method proposed by Santamarina et al. (2002), with the relation (21) where the Methyl Blue Index is VBS, its molecular weight 319.87g/mol., the Avogadro number is A_v and the surface area covered by one methyl blue molecule is A_{MB} (equal to $1.3.10^{-18}m^2$/mol.). The theoretical model of spherical particle allows determination of the theoretical surface of soil S_{part} by unit mass ρ_d which must be divided by φ_a to take into account the real shape of soil particles through relation (22); φ_a is an internal parameter of the model and allows determination of the specific surface of the arrangement with the density of each class (23).

2.12 *Suction linked to the adsorbed water*

The specific surface of the soil which fixes adsorbed water is known with relation (23). Thickness h_a of adsorbed water is measured by Or and Tuller (1999) as a unique function of the mineralogy, water vapor pressure and temperature θ. On a reverse consideration, knowledge of temperature θ and mineralogy allows determination of h_a and the water content linked to the adsorption (24).

Following Frydman and Baker (2009) we assume that the Van Der Waal forces give a suction s equal to the suction of the adsorbed water (25) where S_s is the specific surface of the saturated and unsaturated part of the soil.

$$w_{ads} = S_s.h_a.\rho_w \quad (24)$$

$$s = 10^{-14}/\pi.(S_S/w_{ads})^3 \quad (25)$$

Table 1. The physical parameters of calculation (w) for Wetting path (d) for Drying path on Glass and loam

Sample	Glass	Livet-Gavet	Jossigny
γ_s (kN/m^3)	29	26	27.2
E_p (GPa)	65	107	107
ν_p	0.25	0.2	0.2
e_{Test}	0.667	0.738	0.455
w_r	-	0.27	0.18
θ_c (degree)	20d-25w	0d-5w	0d-5w
R_p (µm)	4 to 140	1.6 to 3mm	0.1 to 0.2mm
T_c (10^{-5}kN/m^3)	7.28	7.28	7.28
MB (cm^3/100g)	0	0.18	4
θ (degree)	20	20	20

3 RESULTS

Simulations of the experiments are made along drying and wetting paths for the relation between the suction and the degree of saturation, with different void ratio and different grading curves. The parameters are shown (Table 1).

3.1 *Graded sample of glass*

The simulation (Fig.10) of the experiment on a graded glass sample (Indarto, 1991) is made with a sample graded between 4-140µm and a unit weight of 18,7kN/m^3. It appears that the new model allows a correct estimation of the experiment curve on the drying path (cor.0.96) and on the wetting path (cor.0.89) to be found. The difference between the new theory and the experiment at 50% of saturation lies between 30kPa on the drying path to 6kPa on the wetting path

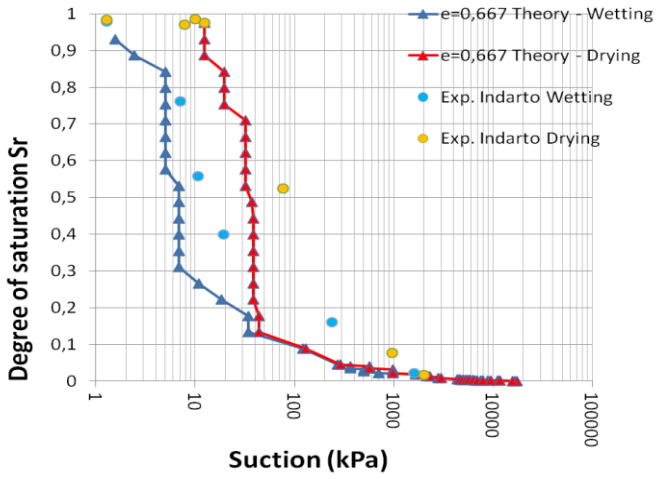

Figure 10. Comparison of theoretical retention curve with the experimental results Indarto (1991); void ratio 0.55; 4µm-140µm diam. glass; wetting angle, 20° at drying 25° at wetting

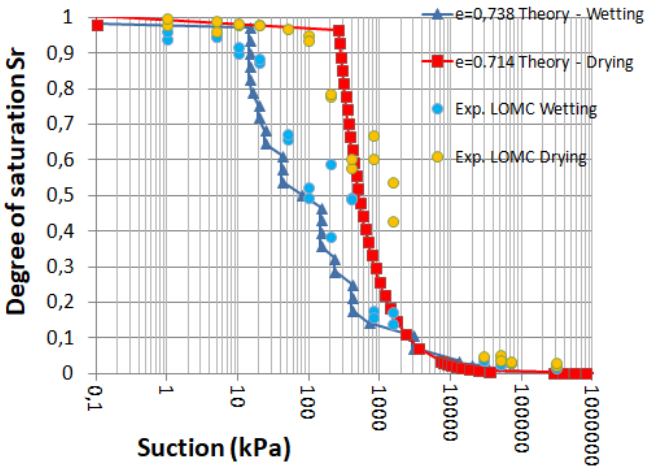

Figure 11. Comparison of the theoretical curve of retention and the experimental results; void ratio 0.71; Livet Gavet Loam; wetting angle, 0° at drying, 5° at wetting

3.2 *Livet-Gavet loam*

The simulation of the Livet-Gavet silt in the form of paste is shown (Fig.11). Particle sizes are between 1.6µm-2mm and density is 15,2kN/m3. The Methyl Blue Index of 0.18 corresponds to a specific surface of 4.4m²/g. The new model allows the experiment curve with a correct correlation on the wetting path

and on the drying path (cor.0.95) to be found. The difference between the new theory and the experiment at 50% of saturation lies between 50kPa on the wetting path to 0kPa on the drying path.

3.3 *Jossigny loam*

The simulation (Fig.12) of the experiment on the Jossigny loam (Fleureau and Indarto, 1993) is made with a sample graded between 0.1µm-0.2mm of density 18kN/m3. This loam is close to a clay with a Methyl Blue Index of 4 which corresponds to a specific surface of 98m²/g. It appears that the new model finds no difference between wetting and drying paths when adsorption prevails with a degree of saturation lower 0.50. For a higher value of saturation, the wetting and drying paths are different. The theory allows a correct estimation of the experiment curve on the wetting path (cor.0.96) and on the drying path (cor.0.99) to be found. The difference between the new theory and the experiment at 50% of saturation lies between 380kPa on the wetting path and cannot be measured on the drying path.

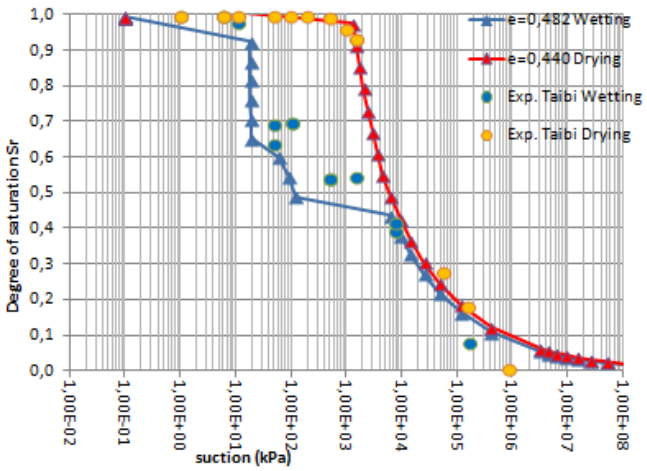

Figure 12. Comparison of the theoretical curve of retention and the experimental results; void ratio 0.48; Jossigny Loam; wetting angle, 0° at drying, 5° at wetting

4 CONCLUSION

A new theory is presented for the retention curve of the soil along drying and wetting path. It explains the difference between these two paths by the saturation of the soil particles with water menisci, which are independent at low saturation, then coalescent at high saturation on the saturation path and by the apparition of air nucleation followed by percolation on the drying path. It shows the difference between the adsorption behavior and the capillarity behavior.

This new model uses only 10 physical parameters (unit mass of solid particle, Young modulus and Poisson ratio of particles, void ratio at the shrinkage limit, water content at shrinkage, particle radius and grading curve, wetting angle, surface tension of water, Methyl Blue Index, temperature) and needs no additional experimental parameters always difficult to determine. It allows the retention curve to be established along the drying and wetting paths. The theoretical retentions curves of the uniform and wide-grained soil clearly show the difference between the drainage and wetting paths, and are very close to the measurements. On the drying path, the model assumes that air will percolate through the soil when bubbles can cross the smallest porosity corresponding to the dominant diameter. The authors would like to thank the financial support provided by the French national project Terre Durable.

5 REFERENCES

Boutonnier L. 2007. Comportement hydromécanique des sols fins proches de la saturation. Cas des ouvrages en terre, *Thèse INPG Grenoble.*

Brooks R.T., Corey A.T 1966. Properties of porous media affecting fluid flows, *Journal Irrigation Drainage Division, ASCE*, 92 (IR2), 61-88.

De Larrard F. 1999. Structure granulaire et formulation des bétons, *Etudes et rech. des LCPC*, OA 34.

Fleureau J.M., Indarto 1993. Comportement du limon de Jossigny remanié soumis à une pression interstitielle négative, *Revue Française Geotechnique*, 62:59-66.

Frydman S., Baker R. 2009. Theoretical soil-water characteristic curves based on adsorption, cavitation, and a double porosity model, *Int. J. Geomech. ASCE*, 9(6):250-256.

Gallipoli D.; Wheeler S.; Karstunen 2003. Modelling the variation of degree of saturation in a deformable unsaturated soil., *Geotechnique*, 53(1):105-112.

Gras J.P. 2011. Approche micromécanique de la capillarité dans les milieux granulaires, *Thèse Univ. Montpellier.*

Indarto 1991. Comportement mécanique et compactage des matériaux de barrage, *Thèse Ecole Centrale Paris.*

Monnet J. , Boutonnier L. 2012. Calibration of an unsaturated Air-Water-Soil model, *Archives of Civil and Mech. Eng.*, 12(4, 5):493-499.

Monnet J., Mahmutovic D., Boutonnier L., Taibi S. 2016. A theoretical retention model for unsaturated uniform and graded soils, *E3S 9 11007 Web of Conf. E-UNSAT 2016, Paris.*

Monnet J., Mahmutovic D., Boutonnier L., Taibi S. 2017. A theoretical retention model for unsaturated soils, *Eur. J. Env. and Civil Eng,*:1-23.

Monnet J., Mahmutovic D., Boutonnier L., Taibi S. , Andrianatrehina R., Branque D., Hoang N.L. 2017. Theoretical Soil Water Characteristic Curves for large graded soil, *Eur. J. Env. and Civil Eng*, :1-35.

Or D., Tuller M. 1999. Liquid retention and interfacial area in variably saturated porous media : upscaling from single pore to sample scale model, *Water Rs. Research*, 35(12):3591-3605.

Santamarina J.C., Klein K.A, Wang Y.H., Prencke E. 2002. Specific surface : determination and relevance, *Can. Geotech. J.* 39 :233-241.

Taibi S. 1994. Comportement mécanique et hydraulique des sols soumis à une pression interstitielle négative, *Thèse Ecole Centrale Paris.*

Van Genuchen 1980. A closed form equation for predicting the hydraulic conductivity of unsaturated soils, Soil Scienc. Soc. Am. J., 44:892-898.